https://doi.org/10.1016/j.ijheatmasstransfer.2019.07.041

Title:

A New Analytical Heat Transfer Model for Deep Borehole Heat Exchangers with Coaxial Tubes

Author:

Aiqiang Pan[a], Lin Lu[a,*], Ping Cui[b,c], Linrui Jia[b,c]

[a] Department of Building Services Engineering, The Hong Kong Polytechnic University, Hong Kong, China

[b]Key Laboratory of Renewable Energy Utilization Technologies in Buildings, Ministry of Education, Jinan, China

[c]School of Thermal Energy Engineering, Shandong Jianzhu University, Jinan, China

Abstract:

Deep borehole heat exchangers (DBHE) provide an effective solution for ground coupled heat pump (GCHP) systems in cold climate region where heating is dominant. Concerning the analytical heat transfer models, the simplification that borehole wall temperature is constant along the depth of ground heat exchangers (GHE) which the existing quasi-three-dimensional models have assumed in the application of shallow borehole GHE, can no longer be accepted in the application of DBHE due to the geothermal gradient in deep ground. Making this simplification cannot give the real temperature distribution of circulating fluid along the depth of DBHE. Therefore, this paper developed a new analytical model for DBHE with coaxial pipes by successfully addressing the increasing borehole wall temperature using the convolution theorem, so that the widely employed quasi-three-dimensional models for shallow borehole GHE is extended for DBHE with coaxial pipes for the first time. The new analytical model is validated by comparing with an existing numerical model. Using the newly developed analytical model, the trends revealing the relationships between thermal performance of DBHE and various parameters are firstly plotted. Because of the high accuracy and quick calculation, this new analytical model can be used as a benchmark

for numerical models. More importantly, the proposed analytical model can be an effective tool for the design and optimization of DBHE, since current numerical models are always calculation-demanding, time-consuming and difficult for engineers and designers to use. Also, the method this paper proposed to address the varying borehole wall temperature can certainly be employed to improve the existing quasi-three-dimensional models for shallow borehole GHE so that they can be applicable in some other cases, for example, GHE installed in layered soils, or affected by underground seepage flow in partial depth.

Key words:

Deep borehole heat exchangers; coaxial tubes; analytical heat transfer model; geothermal gradient; convolution theorem.

Highlights:

1) Firstly developed an analytical model for heat transfer inside deep borehole heat exchangers with coaxial pipes considering the geothermal gradient. The exact temperature distributions of circulating fluid inside deep borehole heat exchanger are firstly calculated using the analytical model.
2) The trends revealing the relationships between thermal performance of deep borehole heat exchangers (i.e. outlet fluid temperature) and various parameters are firstly plotted using the analytical model.
3) The convolution theorem is proposed to address the increasing borehole wall temperature of deep borehole heat exchangers, which is related with geothermal gradients. This method can certainly be employed to improve the existing quasi-three-dimensional analytical models for shallow borehole ground heat exchangers, so that they can be applicable in other cases, for example, GHE installed in layered soils, or affected by underground seepage flow in partial depth.
4) The analytical model is much faster and easier to use than numerical models, and hence can be an effective tool for the design and optimization of ground source heat pump systems with deep borehole heat exchangers. The analytical model can also serve as a benchmark for the accuracy of numerical models.

Nomenclature

z vertical coordinate

Z dimensionless vertical coordinate

r radius

k thermal conductivity

R thermal resistance

R' dimensionless thermal resistance

h convective heat transfer coefficient

Re Reynolds Number

Pr Prandtl Number

Nu Nusselt Number

d hydraulic diameter

l pipe length

μ fluid viscosity

T temperature

Θ dimensionless temperature

M mass flow rate of circulating fluid

c specific thermal capacity

L Laplace transform

s Laplace variable

Subscript

b borehole

p pipe

f circulating fluid

1 outer pipe or space in outer pipe

2 inner pipe or space in inner pipe

o outer radius of pipe

i inner radius of pipe

1. Introduction

1.1 Ground coupled heat pumps & deep borehole heat exchangers

Energy consumption in buildings takes a big proportion of total energy use (about 40%) [1]. Comparing with traditional air source heat pump, ground coupled heat pump (GCHP) systems can save up to 50% energy consumption for space cooling and heating, and providing domestic hot water [2]. This is because the ground is an effective heat source/sink compared with the ambient air. The ground can also be used as thermal storage medium due to its higher thermal capacity, for example, borehole thermal energy storage (BTES) systems [3]. Ground heat exchangers (GHE), as a key component of GCHP systems that interact with the ground, are crucial for system performance. There have been extensive research on different types of GHE, for example, borehole GHE [4], and pile GHE or energy pile [5]. Currently, the most widely used GHE might still be the borehole GHE [6].

In heating or cooling dominant areas, hybrid systems may be required to achieve the ground thermal balance [7]. In recent years, GCHP with deep borehole heat exchangers (DBHE) is found to be an effective solution in cold-climate area where heating is dominant [8]. The depth of ordinary borehole GHE may vary from 50 to 200 meters, whereas DBHE are usually over 1000 meters and may be up to 3000 meters at present. Due to the geothermal gradient (varies around 0.03 ^{o}C/m), DBHE can support a high heating load and sustain for decades' operation [9]. Another difference between shallow borehole GHE and DBHE is the pipe configuration in the borehole. Single U-tube or double U-tubes are usually inserted in shallow borehole GHE, whereas in DBHE, coaxial pipes are generally adopted due to strength issue and construction difficulty.

1.2 Heat transfer models for deep borehole heat exchangers

Both numerical models and analytical models have been established to analyze the heat transfer of shallow vertical GHE [4, 10]. Most of the numerical models are

implemented with commercial software, which are inconvenient for engineers and designers to use for system design and optimization in practical engineering [10]. Analytical models have explicit expressions for calculations of temperature responses. And analytical models are always much faster in calculation compared with numerical models. Analytical models might still be a better tool for design and optimization of GCHP systems.

Currently, most of the models for DBHE are numerical. These numerical models are mostly self-developed rather than based on commercial software [11-15]. The reason that commercial software is not preferred is that the numerical simulation of DBHE involves a wide range of spatial and time scale [16]. The geometry size ranges from millimeters (the thickness of pipes) to thousands of meters (the whole simulation domain), resulting in a considerable number of mesh elements. The time also ranges from minutes to years, requiring a great many of marching steps. Also, to obtain solutions accurate enough, meshing and time steps require sophisticated selection and control. In self-developed numerical simulation, some certain simplifications and specific treatments might be made on the governing heat transfer equations to obtain easier but accurate enough simulation. Nonetheless, numerical modes are not user-friendly to designers and engineers for the design and optimization of GCHP system. Therefore, there is great value in developing analytical models for the application of DBHE.

1.3 Analytical models for heat transfer inside borehole

In analytical analysis of shallow borehole GHE, the heat transfer process is separated into two regions [17]. One is the region outside borehole wall. The widely employed line or cylindrical heat source models are such models that predicting the temperature responses on the borehole wall given the heat flux from the borehole wall. The other is the region inside borehole wall. The analytical models for heat transfer inside borehole wall mainly aim to calculate the outlet fluid temperature given the inlet fluid temperature and the temperature on the borehole wall. This “two regions” methodology has been proved to be effective and widely employed.

The heat transfer inside borehole wall, or the borehole thermal resistance, is a key factor determining thermal performance of borehole GHE. The models for borehole thermal resistance have developed from the original one-dimensional model by Bose [18] to the two-dimensional model by Hellstrom [19], and to the quasi-three-dimensional models by Zeng [17]. Borehole thermal resistance models were systematically summarized by Javed and Spitler [20]. The quasi-three-dimensional models can calculate the temperature change of circulating fluid along the depth of GHE, so that it can take into account the thermal interference (also called thermal "short-circuiting") between the pipes (for example, singe U-tubes and double U-tubes) inside the borehole, which cannot be considered in previous two-dimensional models. This interference is important because it directly affects the performance of borehole GHE.

However, the quasi-three-dimensional models simplified the borehole wall temperature as constant along the depth of the borehole [17]. In the cases of shallow borehole GHE, the initial ground temperature is always seen as uniform. And usually the temperature response at the middle depth of borehole calculated by heat transfer models outside borehole wall (for example, line or cylindrical heat source models) is chosen as the constant borehole wall temperature. For shallow borehole GHE, the constant borehole wall temperature simplification might be acceptable for engineering practice (although the actual borehole wall temperature is not uniform along the depth of the borehole). But in the cases of DBHE, this constant borehole wall temperature simplification cannot be accepted, because the initial temperature of the ground is in no case uniform due to the existence of geothermal gradient. It is just the property that the deep ground has a noticeable increasing temperature that makes DBHE different from shallow borehole GHE. So clearly, the existing quasi-three-dimensional models for shallow borehole GHE cannot be employed for DBHE, not to mention the difference in pipe configuration. The simplification on the borehole wall temperature has resulted in the lack of corresponding analytical models for DBHE as for shallow borehole GHE. Therefore, there's an urgent need of developing analytical models which can take the actual temperature distribution on the borehole wall into account for DBHE with

coaxial tubes.

In this paper, a new analytical model for DBHE with coaxial pipes is developed. This paper extended the existing quasi-three-dimensional analytical models by addressing the simplification on the borehole wall temperature. The exact temperature distribution on borehole wall is accounted using the convolution theorem. With the newly developed model, the parameters affecting the thermal performance of DBHE is systematically analyzed, including flow configuration, thermal conductivity of the grout, inner and outer pipes, radius of inner and outer pipes, mass flow rate of circulating fluid, and geothermal gradient. Besides, the method that this paper newly proposed to treat the actual borehole wall temperature can certainly be employed to improve the existing quasi-three-dimensional analytical models for shallow borehole GHE, since the constant borehole wall temperature simplification also cannot be accepted in some cases, for example, borehole GHE installed in layered soils, and affected by underground seepage flow in partial depth.

2. Model derivation and solution

2.1 Basic assumptions

There are two assumptions or simplifications in the development of the new analytical model for DBHE with coaxial tubes. One assumption is that the thermal capacities of grout and pipes are negligible, since their thermal mass is much smaller than the ground outside the borehole. In this case, the heat transfer process inside borehole is considered as a steady process. This simplification is proved to be valid except for transient analysis within a few hours [21]. This simplification, which has been commonly employed, is convenient for engineering practices. The other simplification is that comparing with the radial heat transfer, the axially conductive heat transfer in the borehole is negligible because of its geometrical characteristics. The two simplifications have also been made by the previous quasi-three-dimensional analytical models [17]. On the other hand, the simplification about borehole wall temperature is no longer adopted in the development of the new analytical model.

2.2 Local thermal resistance

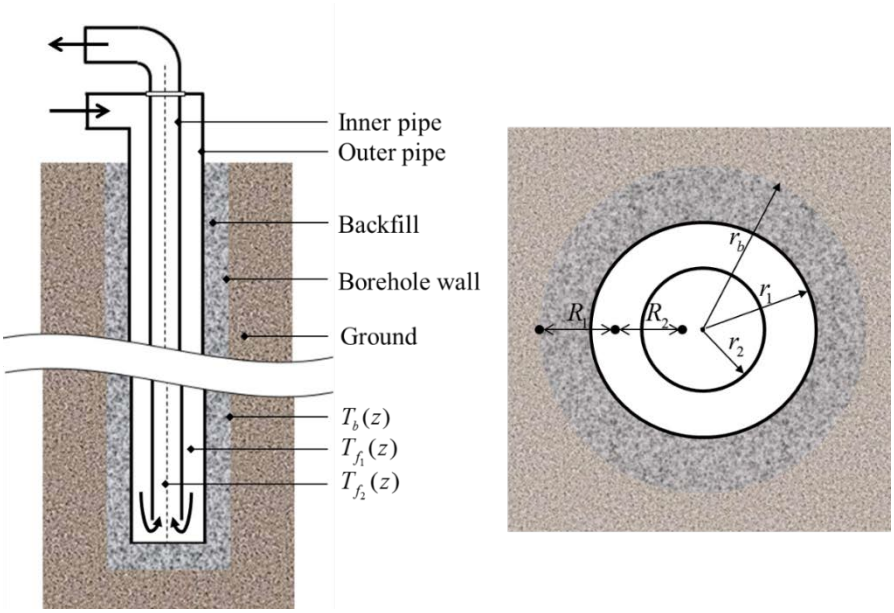

Figure 1 Schematic of deep borehole ground exchangers

In analyzing heat transfer process inside borehole with coaxial tubes, two local

thermal resistances are defined. One is the thermal resistance from borehole wall to fluid in outer pipe (R_1), the other is the thermal resistance from outer pipe fluid to inner pipe fluid (R_2). Their expressions are:

$$R_1 = \frac{1}{2\pi k_b}\ln\left(\frac{r_b}{r_{1o}}\right) + \frac{1}{2\pi k_{p1}}\ln\left(\frac{r_{1o}}{r_{1i}}\right) + \frac{1}{2\pi r_{1i} h_1} \tag{1}$$

$$R_2 = \frac{1}{2\pi r_{2o} h_1} + \frac{1}{2\pi k_{p2}}\ln\left(\frac{r_{2o}}{r_{2i}}\right) + \frac{1}{2\pi r_{2i} h_2} \tag{2}$$

The meaning of the symbols in Equations (1) and (2) can be found in Figure 1. h_1, h_2 are convective heat transfer coefficients for the outer and inner pipe respectively, which can be calculated with Equation (3).

$$h = \frac{k_f}{d} Nu \tag{3}$$

d is the hydraulic diameter. For the inner pipe, d equals the pipe inner diameter $2r_{2i}$. For the outer annular pipe, d equals $2(r_{1i} - r_{2o})$. For the calculation of Nusselt number in case of forced convection in turbulent pipe flow, there are generally three different equations as given in Table 1. The Dittus-Boelter equation is the simplest in form but is not accurate when fluid temperature change is large [22]. In DBHE, the temperature change is considerably larger than in shallow BGHE, so the Dittus-Boelter equation is not suitable for DBHE. The Sieder-Tate equation, as a modified equation of the Dittus-Boelter equation, is more accurate than Dittus-Boelter equation as it takes the change of fluid viscosity with temperature into account (μ_s denotes the fluid viscosity at pipe surface) [22]. In the heat transfer analysis of DBHE, pipe surface temperature changes with depth. But it would be too difficult to solve the governing heat transfer equations when the convective heat transfer coefficients, and hence the local thermal resistances, are functions of temperature. In this paper, the Gnielinski equation is used [22]. The Gnielinski equation has a wider validity range of Reynolds number. It is believed to be more accurate than the previous equations [23]. In the

Gnielinski equation, f is the Darcy-Weisbach friction factor that describes the pipe surface roughness. The Haaland equation is generally used to calculate the Darcy-Weisbach friction factor for circular pipes [24]. For smooth pipes, it has a simpler form $f=\left(0.79\ln(\mathrm{Re})-1.64\right)^{-2}$ [23].

Correlation	Validity
Dittus-Boelter Equation $Nu=0.023\,\mathrm{Re}^{0.8}\,\mathrm{Pr}^{0.4}$	$0.6\le \mathrm{Pr}\le 160$ $\mathrm{Re}>10000$ $l/d>10$
Sieder-Tate Equation $Nu=0.027\,\mathrm{Re}^{0.8}\,\mathrm{Pr}^{1/3}\left(\frac{\mu}{\mu_s}\right)^{0.14}$	$0.7\le \mathrm{Pr}\le 16700$ $\mathrm{Re}>10000$ $l/d>10$
Gnielinski Equation $Nu=\frac{(f/8)(\mathrm{Re}-1000)\,\mathrm{Pr}}{1+12.7(f/8)^{1/2}(\mathrm{Pr}^{2/3}-1)}$	$0.5\le \mathrm{Pr}\le 2000$ $3000\le \mathrm{Re}\le 5\times10^{6}$

Table 1 Calculation of Nusselt Number

2.3 Model derivation

2.3.1 Model for fluid flowing downward through the outer pipe

When the circulating fluid enters DBHE and flows down through outer pipe, and flows out upward through inner pipe, the thermal balance equations for circulating fluid in outer and inner pipes are:

$$Mc\frac{dT_{f_1}(z)}{dz}+\frac{T_{f_1}(z)-T_{f_2}(z)}{R_2}+\frac{T_{f_1}(z)-T_b(z)}{R_1}=0 \tag{4}$$

$$-Mc\frac{dT_{f_2}(z)}{dz}+\frac{T_{f_2}(z)-T_{f_1}(z)}{R_2}=0 \tag{5}$$

The meaning of the symbols in the above equations can be found in Figure 1. The vertical coordinate z is positive downward. The first term in Equation (4) represents the heat transfer of circulating fluid in outer pipe, and the other two terms are radial heat transfer of circulating fluid in outer pipe with grout and with circulating fluid in

inner pipe respectively. The first term in Equation (5) is the heat transfer of circulating fluid in inner pipe, and the other term is radial heat transfer between fluid in inner pipe and fluid in outer pipe. In previous quasi-three-dimensional models, the borehole wall temperature is considered as constant (T_b) along the depth of GHE. In the presented model derivation, the actual borehole wall temperature distribution $T_b(z)$ is kept in model derivation.

The boundary conditions for the thermal balance equations are:

$$\begin{aligned} z = 0 \quad , \quad & T_{f_1}(0) = T_{in} \\ z = z_b \quad , \quad & T_{f_1}(z_b) = T_{f_2}(z_b) \end{aligned} \tag{6}$$

z_b is the depth of borehole. T_{in} is the inlet circulating fluid temperature. The thermal balance equations and boundary conditions can be nondimensionalized with the following dimensionless variables:

$$\Theta_{f_1}(Z) = \frac{T_{f_1}(z)}{T_{in}}, \Theta_{f_2}(Z) = \frac{T_{f_2}(z)}{T_{in}}, \Theta_b(Z) = \frac{T_b(z)}{T_{in}}, Z = \frac{z}{z_b}, R_1' = \frac{McR_1}{z_b}, R_2' = \frac{McR_2}{z_b}$$

So that Equations (4) and (5), and boundary conditions (6) can be expressed in dimensionless form:

$$-\frac{d\Theta_{f_1}(Z)}{dZ} = \frac{\Theta_{f_1}(Z) - \Theta_{f_2}(Z)}{R_2'} + \frac{\Theta_{f_1}(Z) - \Theta_b(Z)}{R_1'} \tag{7}$$

$$\frac{d\Theta_{f_2}(Z)}{dZ} = \frac{\Theta_{f_2}(Z) - \Theta_{f_1}(Z)}{R_2'} \tag{8}$$

$$\begin{aligned} Z = 0 \quad , \quad & \Theta_{f_1}(0) = 1 \\ Z = 1 \quad , \quad & \Theta_{f_1}(1) = \Theta_{f_2}(1) \end{aligned} \tag{9}$$

Apply Laplace transform ($L[f(Z)] = \overline{f}(s)$) with respect to Z on Equations (7) and (8), they become:

$$-s\overline{\Theta}_{f_1}(s) + \Theta_{f_1}(0) = \frac{\overline{\Theta}_{f_1}(s) - \overline{\Theta}_{f_2}(s)}{R_2'} + \frac{\overline{\Theta}_{f_1}(s) - \overline{\Theta}_b(s)}{R_1'} \tag{10}$$

$$s\overline{\Theta}_{f_2}(s) - \Theta_{f_2}(0) = \frac{\overline{\Theta}_{f_2}(s) - \overline{\Theta}_{f_1}(s)}{R_2'} \tag{11}$$

The expressions for $\bar{\Theta}_{f_1}(s)$ and $\bar{\Theta}_{f_2}(s)$ can be solved with the above two equations.

$$\bar{\Theta}_{f_1}(s)=\frac{1}{R_1'R_2's^2+R_2's-1}\left[R_1'(R_2's-1)\Theta_{f_1}(0)+R_1'\Theta_{f_2}(0)+(R_2's-1)\bar{\Theta}_b(s)\right] \quad (12)$$

$$\bar{\Theta}_{f_2}(s)=\frac{1}{R_1'R_2's^2+R_2's-1}\left[(R_1'R_2's+R_1'+R_2')\Theta_{f_2}(0)-R_1'\Theta_{f_1}(0)-\bar{\Theta}_b(s)\right] \quad (13)$$

Then, performing the inverse Laplace transform on Equation (12) and (13), the solutions of temperature distribution in outer and inner pipe can be obtained. In the above two equations, the coefficients of $\Theta_{f_1}(0)$ and $\Theta_{f_2}(0)$ which contain the Laplace variable can be converted directly. However, the expression of borehole wall temperature $\Theta_b(Z)$ after Laplace transform (i.e. $\bar{\Theta}_b(s)$) is not readily known, because $\Theta_b(Z)$, which may be obtained from line or cylindrical heat source model, is already too complex to find the expression after performing Laplace transform $\bar{\Theta}_b(s)$. Not to mention performing the inverse Laplace transform on the expression that $\bar{\Theta}_b(s)$ multiplied by the additionally prefixal term which also contains the Laplace variable s. Fortunately, the convolution theorem of Laplace transform can be employed to address this issue. Let $\bar{G}(s)$ and $\bar{G}'(s)$ denote the coefficients of $\bar{\Theta}_b(s)$ in Equation (12) and (13) respectively. According to the convolution theorem of Laplace transform, the inverse Laplace transform of $\bar{G}(s)\bar{\Theta}_b(s)$ and $\bar{G}'(s)\bar{\Theta}_b(s)$ equal the convolution of their expressions in physical domain.

$$\begin{aligned} L^{-1}[\bar{G}(s)\bar{\Theta}_b(s)] &= G(Z)*\Theta_b(Z) \\ L^{-1}[\bar{G}'(s)\bar{\Theta}_b(s)] &= G'(Z)*\Theta_b(Z) \end{aligned} \quad (14)$$

In Equation (14), the symbol $*$ stands for the convolution operation. The expressions of $G(Z)$ and $G'(Z)$ can be obtained form $\bar{G}(s)$ and $\bar{G}'(s)$ just like the coefficients for $\Theta_{f_1}(0)$ and $\Theta_{f_2}(0)$ in Equations (12) and (13). And $\Theta_b(Z)$ is what is already known by the heat transfer models outside borehole wall. Finally, with the boundary conditions in Equation (9), the solutions of circulating fluid temperature

in outer and inner pipes are:

$$\begin{aligned}\Theta_{f_1}(Z) &= \exp(-\frac{Z}{2R_1'})\left[\cosh(\alpha Z)-\frac{1}{\alpha}(\frac{1}{2R_1'}+\frac{1}{R_2'})\sinh(\alpha Z)\right] \\ &+\exp(-\frac{Z}{2R_1'})\frac{\sinh(\alpha Z)}{\alpha R_2'}\Theta_{f_2}(0)+G(Z)*\Theta_b(Z)\end{aligned} \tag{15}$$

$$\begin{aligned}\Theta_{f_2}(Z) &= -\exp(-\frac{Z}{2R_1'})\frac{1}{\alpha R_2'}\sinh(\alpha Z) \\ &+\exp(-\frac{Z}{2R_1'})\left[\cosh(\alpha Z)+\frac{1}{\alpha}(\frac{1}{2R_1'}+\frac{1}{R_2'})\sinh(\alpha Z)\right]\Theta_{f_2}(0)-G'(Z)*\Theta_b(Z)\end{aligned} \tag{16}$$

Where the expressions for $G(Z)$ and $G'(Z)$ are:

$$\begin{aligned}G(Z) &= \exp(-\frac{Z}{2R_1'})\left[\frac{\cosh(\alpha Z)}{R_1'}-\frac{1}{\alpha}(\frac{1}{R_1'R_2'}+\frac{1}{2R_1'^2})\sinh(\alpha Z)\right] \\ G'(Z) &= \exp(-\frac{Z}{2R_1'})\frac{\sinh(\alpha Z)}{\alpha R_1'R_2'}\end{aligned} \tag{17}$$

The expression for outlet fluid temperature $\Theta_{f_2}(0)$ is:

$$\Theta_{f_2}(0)=\frac{\left[\begin{aligned}&2\alpha R_1'\cosh(\alpha)-\sinh(\alpha) \\ &+2\alpha R_1'\left[G(Z)*\Theta_b(Z)\big|_{Z=1}+G'(Z)*\Theta_b(Z)\big|_{Z=1}\right]\exp(\frac{1}{2R_1'})\end{aligned}\right]}{2\alpha R_1'\cosh(\alpha)+\sinh(\alpha)} \tag{18}$$

And $\alpha=\dfrac{\sqrt{R_2'(4R_1'+R_2')}}{2R_1'R_2'}$.

2.3.2 Model for fluid flowing downward through the inner pipe

When the circulating fluid enters DBHE and flows down through inner pipe and flows out upward through outer pipe, the thermal balance equations for circulating fluid in outer and inner pipes are:

$$\begin{aligned}Mc\frac{dT_{f_2}(z)}{dz}+\frac{T_{f_2}(z)-T_{f_1}(z)}{R_2} &= 0 \\ -Mc\frac{dT_{f_1}(z)}{dz}+\frac{T_{f_1}(z)-T_{f_2}(z)}{R_2}+\frac{T_{f_1}(z)-T_b(z)}{R_1} &= 0\end{aligned} \tag{19}$$

The boundary conditions for the thermal balance equations are:

$$\begin{aligned}z=0 \quad , \quad T_{f_2}(0)&=T_{in} \\ z=z_b \quad , \quad T_{f_1}(z_b)&=T_{f_2}(z_b)\end{aligned} \tag{20}$$

Then, with the same method and procedure, the final solutions of circulating fluid temperature in outer and inner pipes are:

$$\begin{aligned}\Theta_{f_1}(Z) &= \exp(\frac{Z}{2R_1'})\left[\cosh(\alpha Z)+\frac{1}{\alpha}(\frac{1}{2R_1'}+\frac{1}{R_2'})\sinh(\alpha Z)\right]\Theta_{f_1}(0)\\ &-\exp(\frac{Z}{2R_1'})\frac{\sinh(\alpha Z)}{\alpha R_2'}-G(Z)*\Theta_b(Z)\end{aligned} \tag{21}$$

$$\begin{aligned}\Theta_{f_2}(Z) &= \exp(\frac{Z}{2R_1'})\frac{\sinh(\alpha Z)}{\alpha R_2'}\Theta_{f_1}(0)\\ &+\exp(\frac{Z}{2R_1'})\left[\cosh(\alpha Z)-\frac{1}{\alpha}(\frac{1}{2R_1'}+\frac{1}{R_2'})\sinh(\alpha Z)\right]-G'(Z)*\Theta_b(Z)\end{aligned} \tag{22}$$

Where the expressions for $G(Z)$ and $G'(Z)$ are:

$$\begin{aligned}G(Z) &= \exp(\frac{Z}{2R_1'})\left[\frac{\cosh(\alpha Z)}{R_1'}+\frac{1}{\alpha}(\frac{1}{R_1'R_2'}+\frac{1}{2R_1'^2})\sinh(\alpha Z)\right]\\ G'(Z) &= \exp(\frac{Z}{2R_1'})\frac{\sinh(\alpha Z)}{\alpha R_1'R_2'}\end{aligned} \tag{23}$$

The expression for outlet fluid temperature $\Theta_{f_1}(0)$ is:

$$\Theta_{f_1}(0)=\frac{\left[\begin{aligned}&2\alpha R_1'\cosh(\alpha)-\sinh(\alpha)\\&+2\alpha R_1'\left[G(Z)*\Theta_b(Z)\big|_{Z=1}-G'(Z)*\Theta_b(Z)\big|_{Z=1}\right]\exp(-\frac{1}{2R_1'})\end{aligned}\right]}{2\alpha R_1'\cosh(\alpha)+\sinh(\alpha)} \tag{24}$$

3. Model validation

The new analytical model is validated by the numerical model developed by Fang [16]. The parameter values used for model validation are given in Table 2. All the parameters are input parameters for the numerical model. Only the parameters in the upper row are used in the newly developed analytical model. The parameters in the lower row are either not needed (properties outside borehole wall) or neglected (thermal capacity of grout and coaxial pipes) in the analytical model.

As shown in Table 2, the geothermal heat flux is 0.075 W/m^2, and the ground thermal conductivity is 2.5 $W/(m\cdot K)$. With the relation between vertical heat flux and vertical temperature gradient that $\vec{q}_z = -k\frac{\partial T}{\partial z}$, it can be calculated that the original or undisturbed geothermal gradient is 0.03 K/m.

Parameters	Values
borehole depth z_b	2000 (m)
borehole radius r_b	0.140 (m)
outer radius of outer pipe r_{1o}	0.100 (m)
inner radius of outer pipe r_{1i}	0.095 (m)
outer radius of inner pipe r_{2o}	0.070 (m)
inner radius of inner pipe r_{2i}	0.066 (m)
thermal conductivity of grout k_b	1.5 $\left(W/(m\cdot K)\right)$
thermal conductivity of outer pipe k_{p1}	41 $\left(W/(m\cdot K)\right)$
thermal conductivity of inner pipe k_{p2}	0.4 $\left(W/(m\cdot K)\right)$
mass flow rate of water m	12 (kg/s)

thermal capacity of water c	4178 $\left(J/(kg\cdot K)\right)$
geothermal heat flux	0.075 $\left(W/m^2\right)$
average atmosphere temperature	10 (^oC)
convective heat transfer coefficient on ground surface	15 $\left(W/(m^2\cdot K)\right)$
ground thermal conductivity	2.5 $\left(W/(m\cdot K)\right)$
ground thermal diffusivity	1.2×10^{-6} $\left(m^2/s\right)$
volumetric specific thermal capacity of grout	2200 $\left(kJ/(m^3\cdot K)\right)$
thermal capacity of outer pipe	3400 $\left(kJ/(m^3\cdot K)\right)$
thermal capacity of inner pipe	1200 $\left(kJ/(m^3\cdot K)\right)$

Table 2 Parameter values for model validation

The total thermal load of the DBHE is 150 kW . The circulating fluid flows down through the outer pipe and flows back upwards through the inner pipe. After 720 hours' and 1440 hours' operation, the distributions of borehole wall temperature calculated by the numerical model are shown in Figure 2. The borehole wall temperature increases due to the geothermal heat flux. Clearly, using a constant borehole wall temperature to represent the actual borehole wall temperature distribution along the depth of DBHE as assumed by previous quasi-three-dimensional models is not acceptable for DBHE.

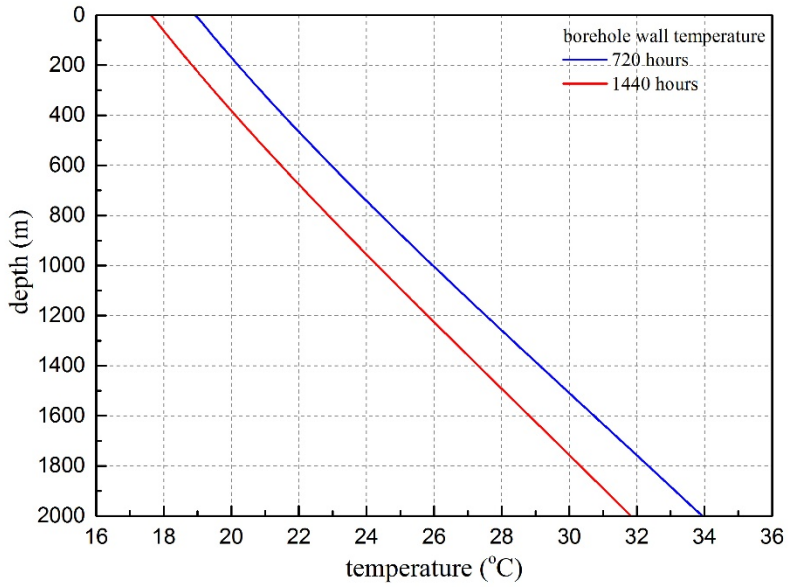

Figure 2 Borehole wall temperature distributions

The borehole wall temperature distributions $T_b(z)$ after 720 and 1440 hours' operation as shown in Figure 2, were converted to dimensionless values $\Theta_b(Z)$ firstly. Then, they were implemented in the analytical model (Equations (15) and (16)) to calculate the circulating fluid temperature distributions in outer and inner pipes along the depth of DBHE. The results are given in Figure 3 and Figure 4 respectively. In both figures, the colored solid lines represent the results of the newly developed analytical model, and the corresponding dash lines stand for the results calculated by the numerical model. The results by the analytical model and numerical model agree well. In both figures, the analytical results are always slightly larger than the numerical results. This may be due to the steady heat transfer assumption (neglecting the thermal capacity of borehole grout and pipes) of the analytical model. However, the relative errors are within 0.6 % and approximately only 0.5 % along the whole depth of DBHE. Therefore, the validity of the analytical model is proved.

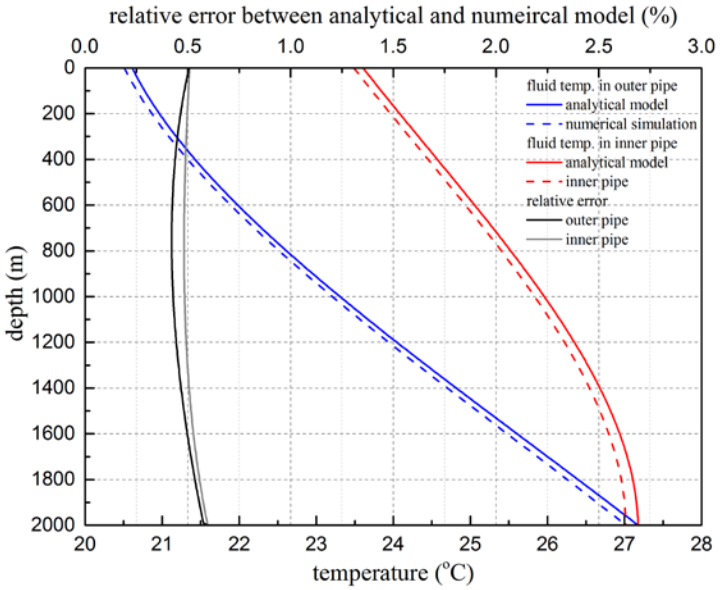

Figure 3 Circulating fluid temperature after 720 hours' operation

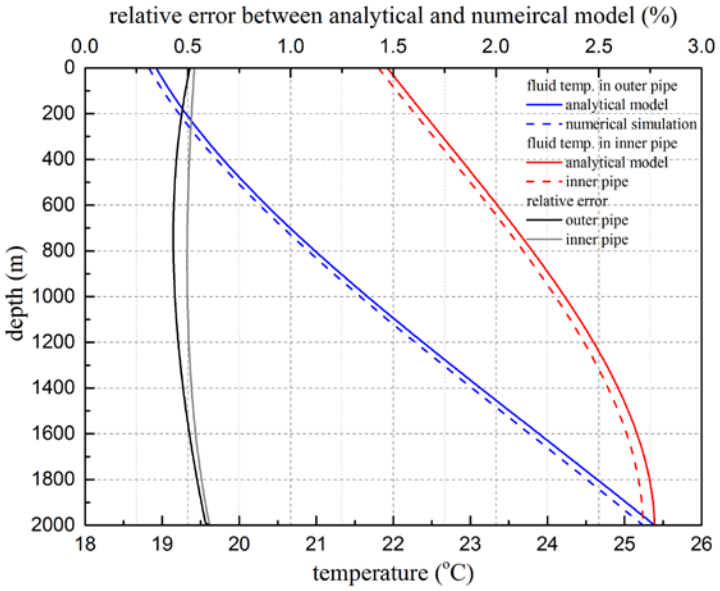

Figure 4 Circulating fluid temperature after 1440 hours' operation

4. Results and analysis

Convenience may be the biggest advantage of the newly developed analytical model. The circulating fluid temperature in the deep borehole can be calculated at the speed of "click-and-done". Therefore, it can be widely employed in practical engineering for the design and optimization of GCHP system with DBHE. Using the newly developed analytical model, the effects of various parameters, including flow configuration, thermal conductivity of borehole grout and pipes, radius of pipes, mass flow rate, and geothermal gradient, on the thermal performance of DBHE are investigated.

It should be pointed out that in our analysis, the pressure drops in the pipes related with the changes of circulating fluid velocity were not considered. Since the pressure drops directly affecting the operational cost of the whole system, the specific pressure drops under different design parameters need additional calculation. In this paper, we provided an effective tool to analyze the thermal aspects of DBHE under various parameters. For the optimization of the whole system, many factors, for example, material costs and operational costs, need to be considered and balanced to obtain the optimal combination of parameters.

4.1 Effect of flow configuration

For the DBHE with coaxial pipes, there are two flow configurations. One is flowing down through the outer pipe and the other is flowing down through the inner pipe. Using the analytical solutions derived above (Equation (15) and Equation (16) for flowing down through the outer pipe; Equation (21) and Equation (22) for flowing down through the inner pipe), the temperature distribution along the depth of DBHE is compared (Figure 5). The parameter values are the same as given in Table 2, and the borehole wall temperature after 720 hours' operation is used.

When the circulating fluid flows down through the outer pipe, the temperature increases from DBHE inlet to bottom is 6.56 ^{o}C, and the temperature decrease from

bottom DBHE to outlet is 3.57 °C. The effective temperature increase (outlet fluid temperature minus inlet fluid temperature) is 3.00 °C. When the circulating fluid flows down through the inner pipe, the temperature increase from DBHE inlet to bottom is only 3.30 °C. When the circulating fluid flow back, the temperature firstly increases to the maximal temperature of 25.38 °C, before further decreasing to 22.33 °C. The effective temperature increase is only 1.82 °C. This difference in effective temperature increase (1.18 °C) is considerably large as the effective temperature increase is only 3.00 °C. Therefore, it can be concluded that the flow configuration that circulating fluid flows down through the outer piper should provide better thermal performance than the other flow configuration.

The outlet temperature difference between two different flow configurations can be directly calculated by Equation (18) minus Equation (24). If the borehole wall temperature in both equations is constant ($\Theta_b = const$) rather than the actual distribution $\Theta_b(Z)$, the subtraction result between Equation (18) and Equation (24) would be zero. This means that when calculating the temperature distribution of circulating fluid for DBHE, assuming a constant borehole wall temperature, as in the previous quasi-three-dimensional models, cannot even respond to the change of flow configuration, which is apparently not real in physics and hence not acceptable.

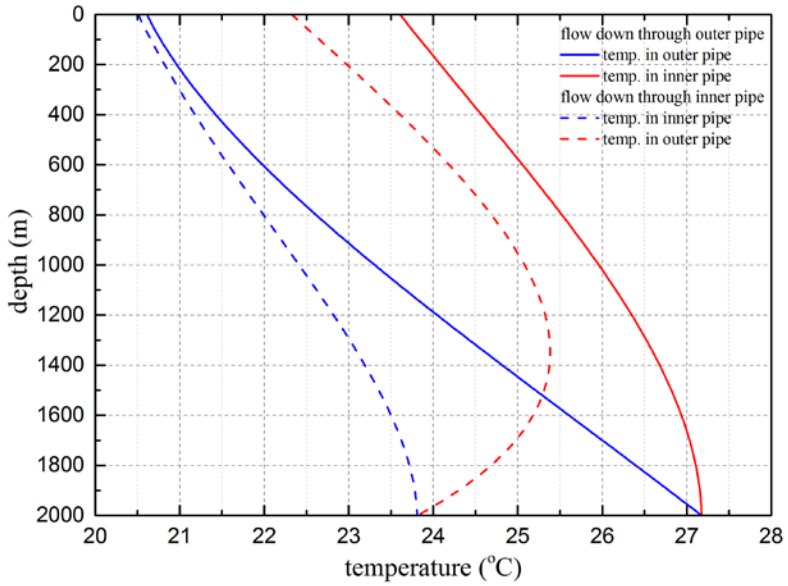

Figure 5 Temperature distribution under different flow configurations

As shown in Figure 5, there is a temperature difference of 0.11 ^{o}C between two blue lines at the inlet. Theoretically, there should not be such a difference at the inlet. The authors want to explain this difference in inlet fluid temperature between the two different flow configurations. For the flow configuration that circulating fluid flows down through the outer pipe, letting Z equals zero, Equation (15) and Equation (16) become Equation (25) and Equation (26) respectively.

$$\Theta_{f_1}(0) = 1 + G(Z) * \Theta_b(Z)\big|_{Z=0} \tag{25}$$

$$\Theta_{f_2}(0) = \Theta_{f_2}(0) \tag{26}$$

For the flow configuration that circulating fluid flows down through the inner pipe, also letting Z equals zero, Equation (21) and Equation (22) becomes Equation (27) and Equation (28) respectively.

$$\Theta_{f_1}(Z) = \Theta_{f_1}(0) - G(Z) * \Theta_b(Z)\big|_{Z=0} \tag{27}$$

$$\Theta_{f_2}(0) = 1 \tag{28}$$

The expressions for $G(Z)$ in Equation (25) and (27) are the expression in Equation (17) and Equation (23) respectively. It can be seen that when circulating fluid flows down through the outer pipe, the dimensionless temperature at the inlet is $1 + G(Z) * \Theta_b(Z)\big|_{Z=0}$ (Equation (25)), whereas the dimensionless temperature at the inlet for the opposite flow configuration is exactly 1 (Equation (28)). The error of 0.11 ^{o}C is caused by $G(Z) * \Theta_b(Z)\big|_{Z=0}$. Although Equation (15) has error in calculating the inlet temperature, Equation (16) is accurate to calculate the outlet temperature. Likewise, although Equation (22) is accurate to calculate the inlet temperature, Equation (21) has error in calculating the outlet temperature. Nonetheless, this error is only 0.44% of the right inlet fluid temperature.

4.2 Effect of thermal conductivity of borehole grout and pipes

4.2.1 Effect of thermal conductivity of borehole grout

To study the effect of the thermal conductivity of borehole grout on the thermal

performance of DBHE, the changes of circulating fluid temperatures at DBHE bottom and outlet with the changes of the thermal conductivity of borehole grout are calculated using the analytical model (Figure 6). The parameter values are the same as given in Table 2 except for the thermal conductivity of borehole grout. The borehole wall temperature distribution after 720 hours' operation is used.

As can be seen from Figure 6, when grout thermal conductivity increases from 0.5 $W/(m\cdot K)$ to 1.5 $W/(m\cdot K)$, the circulating fluid temperature at DBHE bottom increases from 23.85 ºC to 28.88 ºC, and the temperature at DBHE outlet increases from 22.08 ºC to 24.36 ºC. So appearently, the increase in grout thermal conductivity would enhance the thermal performance of DBHE. However, due to the thermal "short-circuiting" between inner and outer pipes, the temperature increase at outlet is smaller (2.28 ºC) compared with that at DBHE bottom (5.03 ºC).

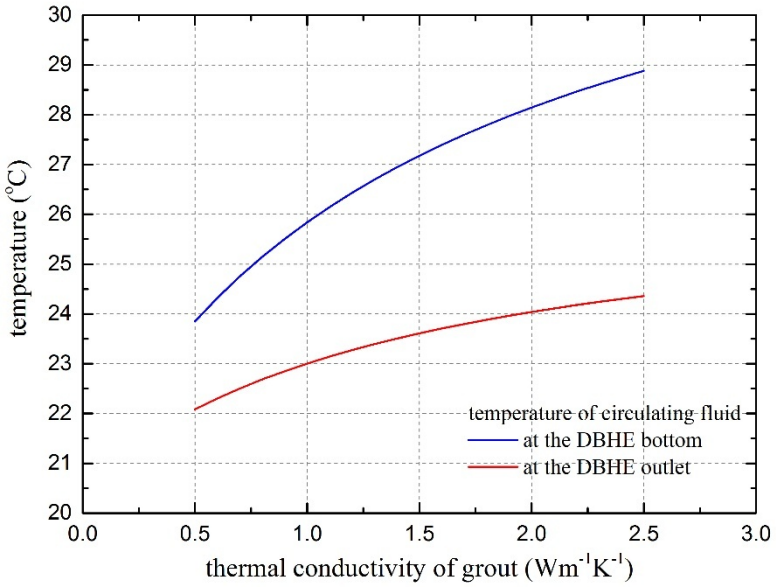

Figure 6 Effect of thermal conductivity of grout

4.2.2 Effect of thermal conductivity of outer and inner pipes

The effect of thermal conductivity of outer and inner pipes are also investigated by letting their values range from values 50 % smaller to values 50 % larger than the original values given Table 2. Other parameter values are kept the same. The changes of circulating fluid temperature at the DBHE bottom and the outlet with the changes of thermal conductivity of outer and inner pipes are given in Figure 7, Figure 8

respectively.

As shown in Figure 7, the circulating fluid temperatures at both the BDHE bottom and outlet barely change with the change of outer pipe thermal conductivity, although the trend of temperature changes are both positive. In contrast, the circulating fluid temperatures at both the BDHE bottom and outlet are more sensitive to the change of inner pipe thermal conductivity as shown in Figure 8. The circulating temperature at DBHE bottom increases from 26.43 ^{o}C to 27.69 ^{o}C when inner pipe thermal conductivity increases from 0.2 $W/(m\cdot K)$ to 0.6 $W/(m\cdot K)$. While the trend for circulating fluid temperature at DBHE bottom is positive, it is negative for the circulating fluid temperature at DBHE outlet. The outlet temperature drops from 24.06 ^{o}C to 23.18 ^{o}C with the same increase of inner pipe thermal conductivity.

The reason for the same positive trend of circulating fluid temperature at DBHE bottom and outlet with the increase of outer pipe thermal conductivity is that higher thermal conductivity of outer pipe means larger ability of extracting heat from outside ground. But the increase of outer pipe thermal conductivity is unlikely to have noticeable effect. Meanwhile, the opposite trend of circulating fluid temperature at DBHE bottom and outlet with the increase of inner pipe thermal conductivity can be explained by the thermal “short-circuiting”. When the inner pipe thermal conductivity is higher, there will be more heat transferred from circulating fluid in the inner pipe to the outer pipe when the circulating fluid flows back upward through inner pipe. And this thermal “short-circuiting” is sensitive to the inner pipe thermal conductivity. Therefore, more efforts or costs should be paid on lowering down the thermal conductivity of inner pipe rather than on increasing the thermal conductivity of the outer pipe.

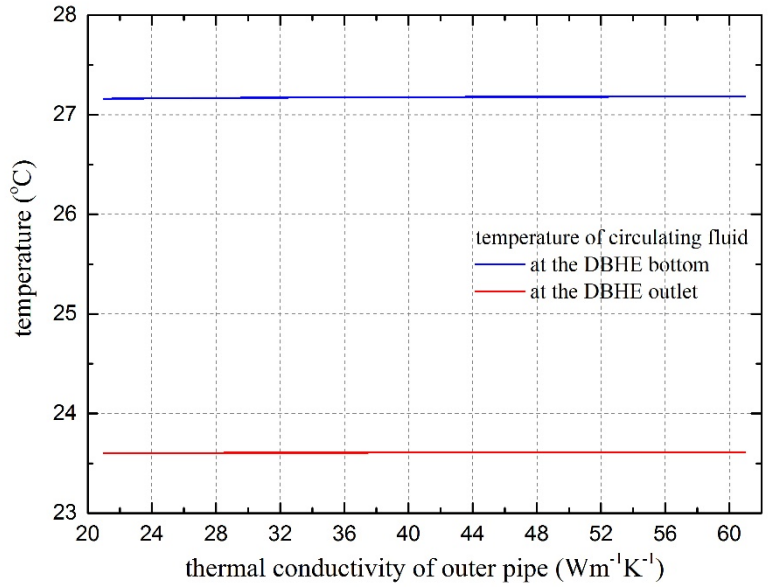

Figure 7 Effect of thermal conductivity of outer pipe

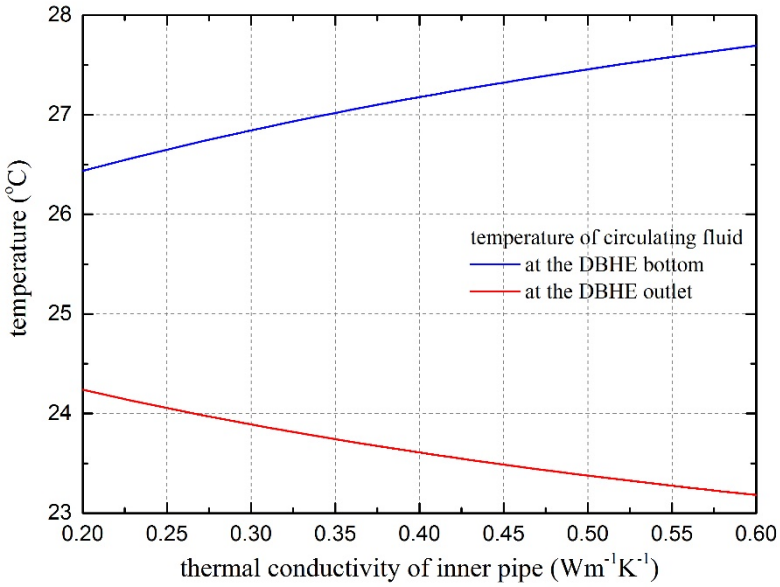

Figure 8 Effect of thermal conductivity of inner pipe

4.3 Effect of pipe radius

The effect of outer and inner pipe radius is investigated by changing the ratio of outer pipe radius to inner pipe radius. The radius ratio given is 10/7 as in Table 2. A smaller ratio and a larger ratio are selected, i.e., 9/8 and 11/6 (when changing the pipe radius, the pipe thickness remains the same). The circulating fluid temperature along the depth of DBHE is shown in Figure 9.

Comparing with the original radius ratio (10/7), when the ratio is smaller (9/8), the

circulating fluid temperatures at DBHE bottom and outlet decrease 0.61 ^{o}C and 0.57 ^{o}C respectively. In contrast, when the ratio is larger (11/6), the corresponding temperature increases 0.84 ^{o}C and 0.79 ^{o}C respectively. It is clear that when the radius ratio of outer to inner pipe is larger, the circulating fluid temperatures at both DBHE bottom and outlet would also be larger.

This may be explained by the changes of heat transfer area of outer and inner pipe with the changes of pipe radius. Since the convective heat transfer amount is proportional to the heat transfer area, larger pipe radius means larger heat transfer area and larger heat transfer amount. When the radius of outer pipe is larger, outer pipe has larger heat transfer area extracting heat from surrounding soil, so the temperature increase at DBHE bottom would be larger. Meanwhile, when the radius of inner pipe is smaller, inner pipe has smaller heat transfer area losing heat to the outer pipe. Therefore, the temperature at DBHE outlet would be higher.

Also, when outer pipe radius is larger and inner pipe radius is smaller, circulating fluid in outer pipe would have relatively lower velocity to have longer time extracting heat from surrounding formation. Meanwhile, circulating fluid in inner pipe would have relatively higher velocity to have shorter time losing heat to the fluid in outer pipe through inner pipe wall. Therefore, increasing the outer pipe radius and reducing the inner pipe radius might be an effective method to enhance the heat extracting ability of DBHE.

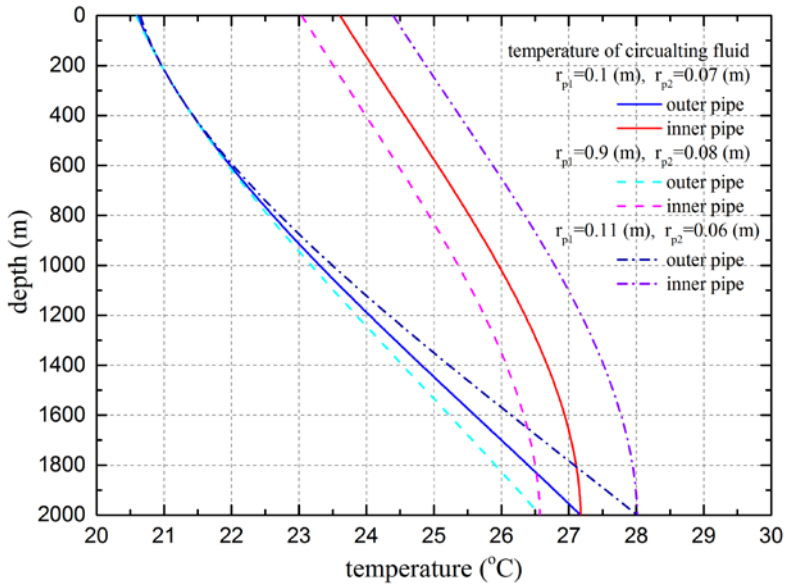

Figure 9 Effect of pipe radius ratio

4.4 Effect of mass flow rate

The effect of mass flow rate on the thermal performance of DBHE is investigated by reducing and increasing the mass flow rate given in Table 2 by 50 %, while other parameters remain the same as given in the table. The temperature distribution on borehole wall after 720 hours' operation is used. The changes of Reynolds numbers and the convective heat transfer coefficients in outer and inner pipes with the changes of mass flow rate are shown in Figure 10. The relationships of circulating fluid temperatures at DBHE bottom and outlet with the mass flow rate are given in Figure 11.

As shown in Figure 10, Reynolds number and the convective heat transfer coefficients all increase with the increase of mass flow rate. Reynolds number in outer pipe ranges from 3.1E4 to 6.1E4, while Reynold number in inner pipe has larger growing rate that increases from 7.7E4 to 15.4E4 approximately. And apparently, Reynolds number in inner pipe is more than two time larger than that in outer pipe. In contrast, although the convective heat transfer coefficients in outer and inner pipe have relatively similar growing rate (from 2600 $W/(m^2 \cdot k)$ to 4700 $W/(m^2 \cdot k)$ and from 2200 $W/(m^2 \cdot k)$ to 3900 $W/(m^2 \cdot k)$ for outer and inner pipe respectively), the

convective heat transfer coefficient of inner pipe is always smaller than that of outer pipe for the same mass flow rate. This probably explains why the flow configuration that circulating fluid flows down through outer pipe provides higher thermal performance. When circulating fluid flows down through inner pipe, it has comparatively less ability (the convective heat transfer coefficient) to extract heat from the surrounding ground. At the same time, when circulating fluid flows upwards through outer pipe, it has comparatively larger ability to lose heat to the surrounding ground.

The circulating fluid temperature at DBHE bottom shows a negative relationship with the increase of mass flow rate as shown in Figure 11. The value drops from 29.01 ^{o}C to 25.87 ^{o}C. In contrast, the temperature at DBHE outlet barely changes with the increase of mass flow rate. The value is 23.60 ^{o}C when mass flow rate equals 8.0 kg/s, and increases marginally to the maximal 23.66 ^{o}C when mass flow increases to 9.8 kg/s, before it keeps decreasing to 23.38 ^{o}C when the mass flow rate further increases to 16 kg/s. The temperature difference of circulating fluid between DBHE bottom and outlet is also plotted in Figure 11. The monotone decrease of temperature difference means that although the circulating fluid in outer pipe can gain more heat under lower flow velocity, the gained heat will not be retained to DBHE outlet, as outlet circulating fluid temperature would not increase likewise. The phenomenon that outlet fluid temperature would remain almost the same with the increase of mass flow rate indicates that DBHE can operate under large mass flow rate condition without significant decrease in outlet temperature. So that more thermal energy can be exploited from DBHE when the mass flow rate is larger.

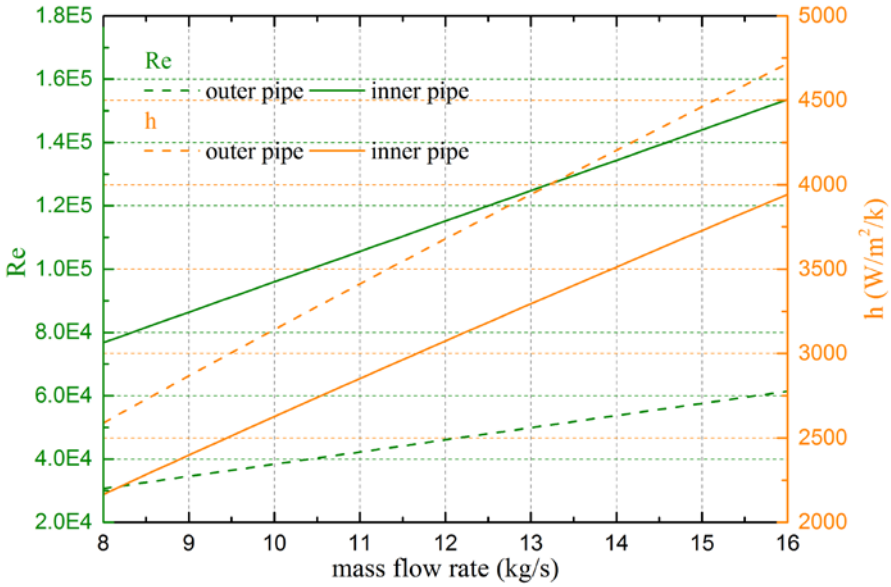

Figure 10 Variation trends of Re and h over mass flow rate

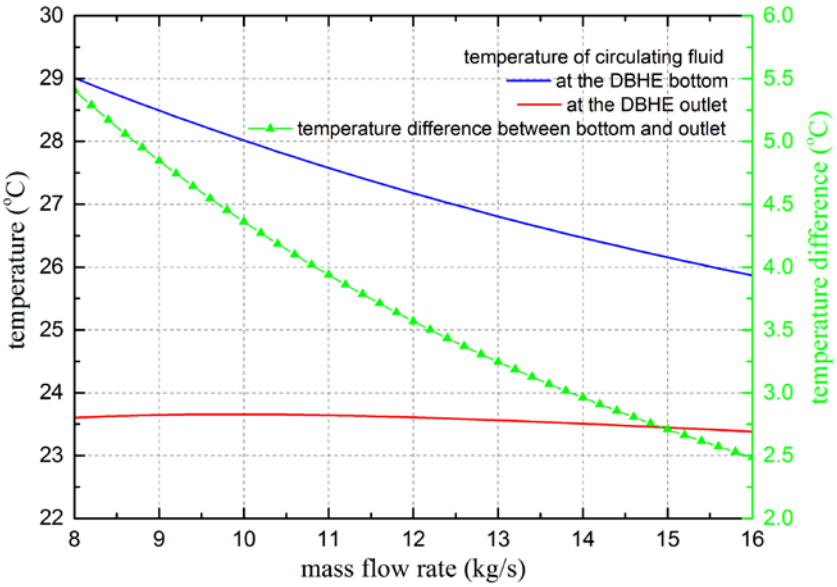

Figure 11 Effect of mass flow rate

4.5 Effect of geothermal gradients

The analysis above all used the same borehole wall temperature after 720 hours' operation when the original geothermal gradient is 0.03 K/m. To show the effect of geothermal effects on the thermal performance of DBHE, three different geothermal gradients (0.02 K/m, 0.03 K/m, and 0.04 K/m) are chosen to calculate the circulating fluid temperature in the DBHE correspondingly. Since the temperature

gradients on borehole wall would decrease with the operation of DBHE, the circulating fluid temperature at the initial stage of operation was calculated. The inlet fluid temperature was set to be 10 ^{o}C. Other parameter values are the same as given in Table 2 in the manuscript. The results are shown in Figure 12.

It can be seen that geothermal gradients have significant impact on the thermal performance of DBHE. When geothermal gradients are 0.02 K/m, 0.03 K/m, and 0.04 K/m respectively, the corresponding circulating fluid temperature at DBHE bottom are 31.48 ^{o}C, 42.20 ^{o}C, and 52.92 ^{o}C. In terms of circulating fluid temperature at DBHE outlet, when geothermal gradient increased from 0.02 K/m to 0.03 K/m, the temperature increased 5.41 ^{o}C. When the geothermal gradient further increased 0.01 K/m, the temperature also increased 5.29 ^{o}C. Therefore, when utilizing geothermal energy with DBHE, the local geothermal gradient would be a key factor determining the thermal performance of DBHE.

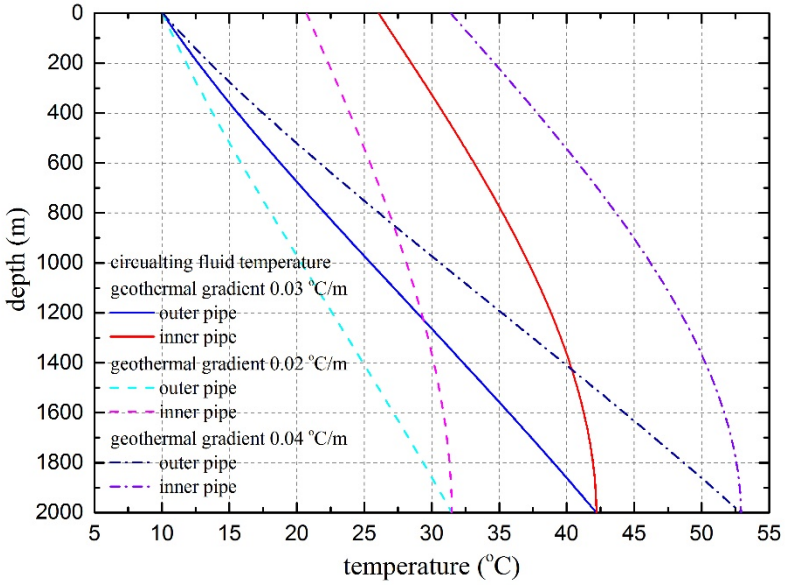

Figure 12 Effect of geothermal gradients

5. Conclusion

In this paper, a new analytical model is proposed for deep borehole heat exchangers (DBHE) with coaxial pipes. The assumption, i.e., assuming a constant borehole wall temperature distribution by the existing quasi-three-dimensional analytical models cannot be accepted for the application of DBHE where borehole wall temperature generally increases with depth due to geothermal gradients. For example, it may unreasonably yield the same value of circulating temperature at DBHE outlet even when the flow configuration is different. In addition, only numerical models for DBHE are reported currently, which are often computation-demanding and time-consuming, making the numerical models inconvenient for designer and engineers to employ for system design and optimization.

This paper found out a novel way to address the increasing borehole wall temperature so that the existing quasi-three-dimensional models are improved to consider the exact temperature distribution. A new analytical model is firstly proposed for DBHE with coaxial pipes. The new analytical model is validated by an existing numerical model. The temperature distributions of circulating fluid along the depth of DBHE calculated by the analytical model shows very good agreement with results by the numerical model. The new analytical model provides an excellent solution for the application of DBHE.

Using the new analytical model, the effects of various parameters on the thermal performance of DBHE (i.e. outlet fluid temperature of DBHE) are investigated. The parameters include flow direction, thermal conductivity of borehole grout and pipes, radius of pipes, mass flow rate, and geothermal gradient. The main valuable conclusions are summarized below:

1) The flow configuration that circulating fluid flows down through the outer pipe and flows back upwards through inner pipe provides better thermal performance of DBHE than the opposite flow configuration. (Figure 5)
2) Increasing borehole grout thermal conductivity would increase the circulating fluid

temperature at both DBHE bottom and outlet and hence improve thermal performance of DBHE. (Figure 6)

3) Changes in the thermal conductivity of outer pipe does not have noticeable effect of circulating fluid temperature at both DBHE bottom and outlet. (Figure 7)
4) Larger thermal conductivity of inner pipe would result in decrease of the circulating fluid temperature at DBHE outlet and hence would result in worse thermal performance, although the temperature at DBHE bottom would be larger. (Figure 8)
5) The radius ratio of outer pipe to inner pipe has a positive relationship with the circulating fluid temperature at both DBHE bottom and outlet, and hence a positive relationship with the thermal performance of DBHE. (Figure 9)
6) The increase of mass flow rate would not bring about significant decrease in the circulating fluid at DBHE outlet. (Figure 11)
7) Local Geothermal gradient is a key factor determining the thermal performance of DBHE. (Figure 12)

Accordingly, the following suggestions are drawn for the application of DBHE based on the conclusions above:

1) The flow configuration that circulating fluid flows down through outer pipe is suggested.
2) Concerning the construction materials, more attentions should be paid on improving thermal conductivity of borehole grout and lowering thermal conductivity of inner pipe, rather than on that of outer pipe.
3) Concerning the radiuses, larger outer pipe radius and smaller inner pipe radius are preferred.
4) DBHE can be designed to operate with large mass flow rate without significant decrease in energy output.

The rapid calculation (“click and done”) feature of the new analytical model makes it an effective tool for the application of DBHE. And the model can be used as a benchmark for validating and checking the accuracy of numerical models. Also, the method (convolution theorem) presented in this paper to address the exact temperature

distribution on borehole wall can certainly be employed for the application of shallow GHE to improve the accuracy of calculating GHE outlet fluid temperature of, since the constant borehole wall temperature assumption, as assumed by the existing quasi-three-dimensional model is only a simplification but not for real cases. For example, the temperature near ground surface can be considerably different. The temperature in different soil layers can also be different. When the ground seepage flow only exists in some depth range of borehole GHE, the temperature distribution would also be different.

Furthermore, we would like to mention that the borehole wall temperatures we used in this research were obtained from the numerical model. To calculate the borehole wall temperature for the application of DBHE, the existing line heat source model for shallow borehole GHE, which assumes a constant heat transfer rate along borehole, needs to be improved to address the issue of changing heat transfer rate along the depth of borehole. This could be another research point in the next stage.

Reference

1. Atam, E. and L. Helsen, *Ground-coupled heat pumps: Part 1–Literature review and research challenges in modeling and optimal control.* Renewable and Sustainable Energy Reviews, 2016. **54**: p. 1653-1667.
2. Sarbu, I. and C. Sebarchievici, *General review of ground-source heat pump systems for heating and cooling of buildings.* Energy and buildings, 2014. **70**: p. 441-454.
3. Rapantova, N., et al., *Optimisation of experimental operation of borehole thermal energy storage*. Applied Energy, 2016. **181**: p. 464-476.
4. Yang, H., P. Cui, and Z. Fang, *Vertical-borehole ground-coupled heat pumps: A review of models and systems.* Applied Energy, 2010. **87**(1): p. 16-27.
5. Fadejev, J., et al., *A review on energy piles design, sizing and modelling.* Energy, 2017.
6. Rees, S.J., *An introduction to ground-source heat pump technology*, in *Advances in Ground-Source Heat Pump Systems*. 2016, Elsevier. p. 1-25.
7. Drosou, V.N., et al., *The HIGH-COMBI project: High solar fraction heating and cooling systems with combination of innovative components and methods.* Renewable and Sustainable Energy Reviews, 2014. **29**: p. 463-472.
8. Sapinska-Sliwa, A., et al., *Deep borehole heat exchangers—A conceptual and comparative review.* International Journal of Air-Conditioning and Refrigeration, 2016. **24**(01): p. 1630001.
9. Holmberg, H., et al. *Deep borehole heat exchangers, application to ground source heat pump systems*. in *Submitted to the World Geothermal Congress*. 2015.
10. Li, M. and A.C. Lai, *Review of analytical models for heat transfer by vertical ground heat exchangers (GHEs): A perspective of time and space scales.* Applied Energy, 2015. **151**: p. 178-191.
11. Song, X., et al., *Numerical analysis of heat extraction performance of a deep coaxial borehole heat exchanger geothermal system.* Energy, 2018. **164**: p. 1298-1310.
12. Song, X., et al., *Heat extraction performance of a downhole coaxial heat exchanger geothermal system by considering fluid flow in the reservoir.* Geothermics, 2018. **76**: p. 190-200.
13. Le Lous, M., et al., *Thermal performance of a deep borehole heat exchanger: Insights from a synthetic coupled heat and flow model.* Geothermics, 2015. **57**: p. 157-172.
14. Holmberg, H., et al., *Thermal evaluation of coaxial deep borehole heat exchangers.* Renewable energy, 2016. **97**: p. 65-76.
15. Wang, Z., et al., *Field test and numerical investigation on the heat transfer characteristics and optimal design of the heat exchangers of a deep borehole ground source heat pump system.* Energy Conversion and Management, 2017. **153**: p. 603-615.
16. Fang, L., et al., *A computationally efficient numerical model for heat transfer simulation of deep borehole heat exchangers.* Energy and Buildings, 2018. **167**: p. 79-88.
17. Zeng, H., N. Diao, and Z. Fang, *Heat transfer analysis of boreholes in vertical*

ground heat exchangers. International Journal of Heat and Mass Transfer, 2003. **46**(23): p. 4467-4481.
18. Bose, J.E., *Design/data manual for closed-loop ground-coupled heat pump systems.* ASHRAE, 1985.
19. Hellstrom, G., *Ground heat storage: Thermal analyses of duct storage systems. I. Theory.* 1992.
20. Javed, S. and J.D. Spitler, *Calculation of borehole thermal resistance*, in *Advances in Ground-Source Heat Pump Systems*. 2016, Elsevier. p. 63-95.
21. Yavuzturk, C., J.D. Spitler, and S.J. Rees, *A transient two-dimensional finite volume model for the simulation of vertical U-tube ground heat exchangers*. ASHRAE transactions, 1999. **105**(2): p. 465-474.
22. *https://www.nuclear-power.net/nuclear-engineering/heat-transfer/convection-convective-heat-transfer/dittus-boelter-equation/*.
23. Incropera, F.P., et al., *Fundamentals of heat and mass transfer*. 2007: Wiley.
24. Massey, B.S. and J. Ward-Smith, *Mechanics of fluids*. Vol. 1. 1998: Crc Press.